



Bright Polarized Single-Photon Source Based on a Linear Dipole

S. E. Thomas, M. Billard, N. Coste, S. C. Wein, Priya Priya, H. Ollivier, O. Krebs, L. Tazaïrt, A. Harouri, A. Lemaître, et al.

► To cite this version:

S. E. Thomas, M. Billard, N. Coste, S. C. Wein, Priya Priya, et al.. Bright Polarized Single-Photon Source Based on a Linear Dipole. 2020. hal-03059771

HAL Id: hal-03059771

<https://cnrs.hal.science/hal-03059771>

Preprint submitted on 14 Dec 2020

HAL is a multi-disciplinary open access archive for the deposit and dissemination of scientific research documents, whether they are published or not. The documents may come from teaching and research institutions in France or abroad, or from public or private research centers.

L'archive ouverte pluridisciplinaire **HAL**, est destinée au dépôt et à la diffusion de documents scientifiques de niveau recherche, publiés ou non, émanant des établissements d'enseignement et de recherche français ou étrangers, des laboratoires publics ou privés.

Bright Polarized Single-Photon Source Based on a Linear Dipole

S. E. Thomas¹, M. Billard², N. Coste^{1,2}, S. C. Wein³, Priya¹, H. Ollivier¹, O. Krebs¹, L. Tazaïrt¹, A. Harouri¹, A. Lemaitre¹, I. Sagnes¹, C. Anton¹, L. Lanço^{1,4}, N. Somaschi², J. C. Loredo^{*,1}, and P. Senellart^{+,1}

¹*Centre for Nanosciences and Nanotechnology, CNRS, Université Paris-Saclay,
UMR 9001, 10 Boulevard Thomas Gobert, 91120, Palaiseau, France*

²*Quandela SAS, 10 Boulevard Thomas Gobert, 91120, Palaiseau, France*

³*Institute for Quantum Science and Technology and Department of Physics and Astronomy,
University of Calgary, Calgary, Alberta, Canada T2N 1N4*

⁴*Université Paris Diderot - Paris 7, 75205 Paris CEDEX 13, France*

* email: juan.loredo1@gmail.com

+ email: pascale.senellart-mardon@c2n.upsaclay.fr

Semiconductor quantum dots in cavities have emerged as high-performance single-photon sources for quantum technologies [1–4]. However, they are still far from ideal deterministic operation, which simultaneously requires perfect linear polarization, population inversion and collection efficiency [3]. Thus far, the best performing sources have used an unpolarized emitter together with polarized photon extraction [2, 5, 6]. Here, we explore a new path to deterministic operation: exploiting the natural asymmetry of neutral quantum dots that present linearly-polarized dipoles and allow for the emission of fully polarized light. To benefit from such a property, we propose the use of off-resonant phonon-assisted excitation that has been theoretically predicted to enable near-unity population inversion and quantum purity [7–9]. We experimentally study this approach for quantum dots in micropillar cavities and demonstrate single-photon emission with a degree of linear polarization up to 0.994 ± 0.007 and a high population inversion – 85% as high as resonant excitation. We demonstrate a single-photon source with a polarized first lens brightness of 0.51 ± 0.01 , a single-photon purity of 0.939 ± 0.001 and single-photon indistinguishability of 0.915 ± 0.003 .

The path towards an optimal single-photon source requires finding a scheme in which single photons are generated in a well-defined spatial and polarization mode, with near-unity efficiency, purity and indistinguishability. A device with these properties is highly sought-after for the advancement of quantum technologies such as secure long-distance quantum communication [10] and quantum computing [11–13]. Several platforms towards optimised single-photon sources are being developed, including spontaneous parametric down-conversion (SPDC) [14–16] and four-wave mixing (FWM) [17, 18]. These non-linear optical sources have an intrinsic efficiency limitation, and various multiplexing schemes are currently being explored to overcome this [18–22]. Sources based on semiconductor quantum dots (QDs) in microcavities have recently shown their capability to deliver high purity, indistinguishable single photons with record brightness [1, 2, 5, 23]. With an efficiency per photon more than one order of magnitude higher than sources based on frequency conversion, QD sources have already allowed a substantial scaling up of optical quantum computing [4].

Despite this impressive progress, current QD sources are still far from the ideal deterministic performance that would provide a single photon in a pure quantum state with unity probability. This ambitious goal requires a full inversion of the QD transition that emits a single photon with near-unity probability and quantum purity, and that the photon is perfectly collected into a well-defined polarized optical mode. Coherent control of a QD has

allowed generation of single photons in pure quantum states [24], and near-unity population inversion has been obtained through more sophisticated techniques such as rapid adiabatic passage [25, 26]. Unpolarized collection efficiencies in the 60–78% range have been demonstrated with micropillar cavities [1, 2]. However, obtaining such high performance into a polarized mode remains challenging. So far, the most efficient sources have used resonant excitation of a charged exciton state, which inherently emits unpolarized photons. Using unpolarized cavities, only half of the single photons are collected through polarization filtering [1, 2, 6]. Very recently, polarized cavities were used to accelerate spontaneous emission into one linear polarization providing a factor of two gain in the source efficiency [5, 27]. However, it is unclear whether such method could provide near-unity polarization degree.

Here, we propose a new path towards deterministic operation – making use of the natural asymmetry of a neutral QD whose eigenstates present linearly-polarized optical transitions. Such an approach allows for fully polarized single photon emission. To benefit from this attractive feature, we implement a near off-resonant phonon-assisted excitation scheme that has recently been theoretically proposed to reach both high QD inversion probability and high quantum purity [7–9]. The unique combination of these ingredients allows us to report on a source of nearly-perfectly polarized single photons with state-of-the-art performance.

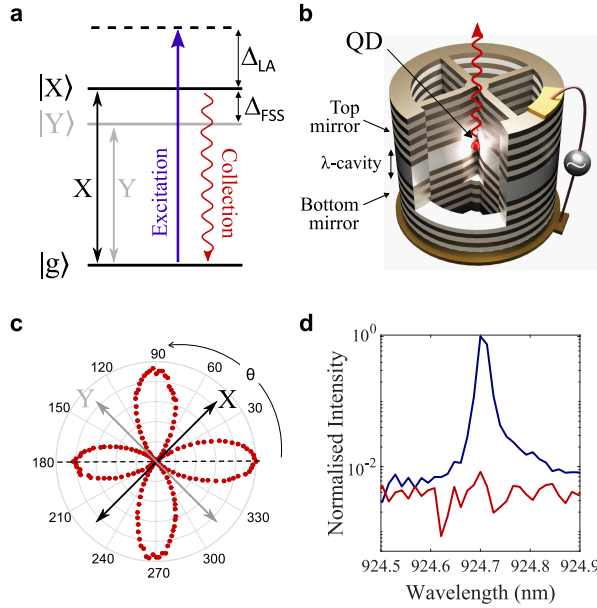


FIG. 1. Proposed scheme for high-efficiency linearly polarized single photon source. (a) Energy level structure of a neutrally charged quantum dot, with ground state $|g\rangle$ and two exciton eigenstates $|X\rangle$ and $|Y\rangle$, separated in energy by the fine structure splitting Δ_{FSS} . The longitudinal acoustic (LA) phonon assisted excitation scheme uses an excitation pulse blue-detuned from the transition by an energy of Δ_{LA} , or equivalently detuned in wavelength by $\Delta\lambda$, and is aligned in polarization along the X dipole. (b) A schematic of the quantum dot deterministically embedded at the centre of an electrically-contacted micropillar cavity [1]. (c) Polar plot of the cross-polarized emission intensity measured under phonon-assisted excitation as a function of the incident polarization angle. (d) Spectrum of the emitted photons when exciting only the X dipole of a neutral exciton and collecting in the parallel (blue) or orthogonal (red) basis, plotted on a log scale. The off-resonant LA-phonon-assisted excitation is detuned by $\Delta\lambda=0.6$ nm and has a pulse duration of 19 ps.

We exploit the optical selection rules of a neutral InGaAs QD to directly generate linearly polarized single photons. Self-assembled quantum dots present a shape asymmetry, both in the growth direction and transversely, that reduces the system symmetry to C_{2v} . This leads to a three-level structure in neutral QDs as shown in Fig. 1(a) where two excitonic eigenstates, labelled $|X\rangle$ and $|Y\rangle$, are separated by the fine structure splitting, Δ_{FSS} , which is determined by the valence band mixing and Coulomb exchange interaction [28]. The optical transition between the QD ground state $|g\rangle$ and one of the exciton states corresponds to a linearly-polarized dipole. While optical quantum technologies require polarized single photons, direct use of such a linear dipole has not been considered so far. Indeed, the generation of single photons with near-unity indistinguishability has only been reached under resonant excitation, a technique which is not applicable to a single linear dipole. In such

a case, the single photons present the same wavelength and polarization as the excitation laser and cannot be easily separated.

To overcome this limitation, we propose the use of a phonon-assisted excitation scheme, making use of a slightly spectrally-detuned laser that can be easily separated from the single photons. This excitation scheme was recently introduced [7, 29] and relies on a detuned strong optical pulse that dresses the ground and excited states of the optical transition. During the pulse duration, a strong occupation of the excited state is obtained through an adiabatic undressing mediated by the emission of longitudinal-acoustic (LA) phonons. After the first observation of such phonon-assisted excitation [30], further theoretical studies predicted this excitation scheme should also provide near-unity single-photon purity, indistinguishability and occupation probability [8, 9]. The combination of this phonon-assisted excitation scheme with the use of a QD linear dipole thus appears as a promising route toward near-deterministic single photon sources.

We study several devices consisting of a QD deterministically located at the center of an electrically connected micropillar cavity (Fig. 1(b)) [1]. These devices have previously been shown to provide reproducible, high-performance single-photon generation under strictly resonant excitation, where the excitation laser was separated from the emitted photons via cross-polarisation. This reduced the polarized collection efficiency by a factor of two, and the polarized source brightness \mathcal{B}_{FL} , i.e. the probability to collect a polarized single photon per pulse, to around $\mathcal{B}_{\text{FL}} \approx 25\%$ [1, 6]. In the present work, the laser is blue-detuned from the QD transition by approximately 0.6 nm, corresponding to a phonon energy of around 1 meV. The single photons are separated from the pump laser using spectral filters (see Methods).

We can visualize the two linear dipoles of the neutral QD, by measuring the single photon emission in the orthogonal polarization to the excitation laser. The corresponding intensity when varying the excitation polarization direction is shown in Fig. 1(c). The intensity in cross polarisation goes to zero when the polarization is aligned along one of the exciton linear dipoles and increases in between. In the following, only one of the excitonic dipoles is excited, and the system reduces to an effective two-level system, $\{|g\rangle, |X\rangle\}$. The measured spectra of the single photons when collecting parallel or orthogonal to the X polarization direction, are shown in Fig. 1(d), evidencing strongly polarized emission. By calculating the integrated intensity measured in parallel (crossed) polarization I_{\parallel} (I_{\perp}), we find a degree of linear polarization, $D_{\text{LP}} = \frac{I_{\parallel} - I_{\perp}}{I_{\parallel} + I_{\perp}} = 0.994 \pm 0.007$ for device A1 on Sample A (see Methods). The same measurement was performed for two further different exciton-based devices on Sample A (devices A2 and A3) demonstrating linear polariza-

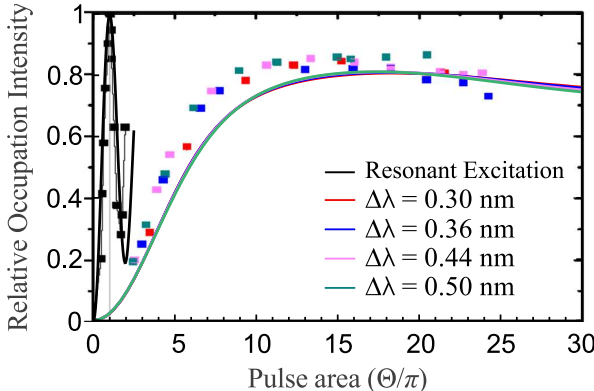


FIG. 2. **Occupation probability via the phonon-assisted excitation scheme.** Measured intensity of single-photon emission from a charged exciton collected in cross-polarization for resonant excitation and LA-phonon-assisted excitation at various detunings $\Delta\lambda$. The emission intensity is normalized to the maximum achieved under resonant excitation to allow comparison between the two schemes. The error bars are within the size of the plotted points. The solid lines give the theoretical prediction based on the model in [9].

tion degree D_{LP} of 0.981 ± 0.004 and 0.971 ± 0.001 . This polarization degree significantly exceeds what is accessible using polarized Purcell effect in asymmetric cavities, with maximal values of 0.93 in optimized structures [5] – a limitation that arises from a compromise between reducing the cavity linewidth (to obtain large cavity splitting to linewidth ratios), and remaining in the weak coupling regime. With the current approach, there is no fundamental limit to the degree of polarization that could be reached. Even if the two linear dipoles present a slight non-orthogonality, which arises when the quantum dot shape and strain anisotropies do not coincide [31, 32], it is always possible to excite a single dipole by aligning the excitation light to be orthogonal to the other dipole axis.

We now investigate the QD occupation probabilities p_{QD}^{LA} that can be obtained through LA-phonon-assisted excitation. In practice, the measurement of this absolute value is a significant experimental challenge that would require precise estimation of the many parameters governing the single photon emission intensity (see Supplementary Material). It is more instructive to measure the relative occupation probability reachable with phonon-assisted excitation, compared to the one achieved under resonant excitation p_{QD}^{LA}/p_{QD}^{RF} . To do so, we compare the single photon emission in a cross-polarisation configuration, to be able to separate single photons from the laser for both excitation schemes. We study a charged exciton on Sample B (see Methods), which corresponds to a four-level system that acts as an effective two-level system when collecting the emission in cross-polarization [6]. Fig. 2 presents the single-photon counts detected under strictly resonant excitation (black) and using LA-phonon-assisted excitation (coloured) for a pulse dura-

tion of 19 ps and various laser detunings as a function of the pulse area experienced by the quantum dot. The pulse area is proportional to the square root of the intracavity power, which is obtained by correcting from the cavity transmission when the laser energy is detuned from the optical resonance. The resonant excitation data exhibits well-known Rabi oscillations reflecting the coherent control of the optical transition. Conversely, the LA-phonon-assisted excitation scheme does not show oscillations but a single rise and then slow decrease of the signal. Solid lines show the theoretical predictions based on the model presented in [9] for the parameters corresponding to our experimental situation. Theory and experiment are in good agreement and show the occupation probability under LA-phonon-assisted excitation is as large as 0.85 ± 0.01 compared to that reached under resonant excitation. Such high occupation probability is also observed on device A3 as shown below. Theory indicates that the QD occupation probability could be brought closer to unity using lower temperature and developing appropriate temporal shaping of the excitation laser [29].

We next investigate the single-photon purity and indistinguishability of the collected photons. We measure the second-order autocorrelation, $g^{(2)}(0)$, and the Hong-Ou-Mandel interference visibility, V_{HOM} , for various excitation conditions for device A3, and typical results are shown in Fig. 3(a) (see Methods for more details). When using an excitation pulse which is detuned from resonance by $\Delta\lambda = 0.6 \text{ nm}$ and has a pulse duration of $\tau = 19 \text{ ps}$, we observe $g^{(2)}(0) = 0.057 \pm 0.001$ and $V_{HOM} = 0.810 \pm 0.004$, from which we extract a single-photon purity of $\mathcal{P} = 1 - g^{(2)}(0) = 0.943 \pm 0.001$ and a single-photon mean wavepacket overlap [33] of $M_s = 0.920 \pm 0.005$. As a comparison, the same measurements are performed in the standard resonance fluorescence (RF) excitation scheme, rejecting the laser component via cross polarization. In this case, the polarization of the excitation pulse is aligned along one of the cavity axes and the laser excites a combination of both X and Y optical transitions [6]. At π -pulse excitation, we measure $g^{(2)}(0) = 0.011 \pm 0.001$, and $M_s = 0.915 \pm 0.001$, showing that the indistinguishability under the LA-phonon-assisted excitation scheme is the same to that obtained from resonant excitation. The higher $g^{(2)}(0)$ in the LA-phonon-assisted excitation scheme is partly due to re-excitation of the QD for the pulse duration of 19 ps used here (see Supplementary Material). We find that these values further improve to $g^{(2)}(0) = 0.011 \pm 0.001$ and $M_s = 0.948 \pm 0.001$ for the LA-phonon-assisted excitation and to $g^{(2)}(0) = 0.009 \pm 0.001$, and $M_s = 0.962 \pm 0.004$ for resonant excitation when adding an additional 10 pm bandwidth etalon in the collection path. This additional spectral filtering reduces the phonon sideband emission, as well as any extra spectrally-broader photons, thus improving the single-photon purity and indistinguishabil-

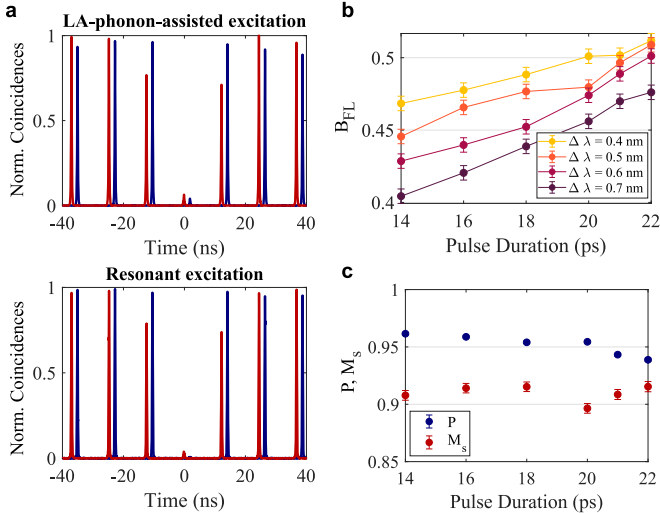


FIG. 3. Source Performance (a) Comparison of the measured $g^{(2)}(0)$ (blue) and HOM interference (red) for the LA-phonon-assisted (upper) and resonant (lower) excitation schemes. The $g^{(2)}(0)$ data is offset horizontally by 2 ns for clarity. For LA-phonon-assisted excitation the laser is detuned by $\Delta\lambda = 0.6$ nm from resonance. For both schemes, the pulse has a duration of $\tau = 19$ ps, and the power is chosen to maximise the emitted photon rate. (b) The first lens brightness, B_{FL} , as a function of the detuning, $\Delta\lambda$, and the pulse duration, τ . (c) The single-photon purity, $P = 1 - g^{(2)}(0)$, and the single-photon indistinguishability, M_s , as a function of the pulse duration, τ , of LA-phonon-assisted excitation with a detuning of $\Delta\lambda = 0.4$ nm. In all cases, the values are obtained for a power maximizing the occupation probability.

ity for both excitation schemes [34]. We note that recently, an indistinguishability of 80% was observed for both phonon-assisted and resonant excitation for GaAs QDs [35]. Our work shows for the first time that near-unity indistinguishability can be reached using phonon-assisted excitation as theoretically predicted.

Finally, to evaluate the overall performance of a single-photon source based on an excitonic linear dipole under LA-phonon-assisted excitation, we measure the polarized brightness, single-photon purity and indistinguishability of device A3 as a function of the detuning, $\Delta\lambda$, and pulse duration of the excitation laser, τ . For each set of parameters, we adjust the excitation power to reach maximum brightness. In order to evaluate the first lens brightness, B_{FL} , we precisely calibrate all losses and the detector efficiency of our experimental setup, see Supplementary Material for a detailed loss budget. Fig. 3(b) shows that higher brightness is achieved for smaller detunings, and Fig. 3(c) shows the source performances as a function of the pulse length for a detuning of $\Delta\lambda = 0.4$ nm. Single-photon indistinguishabilities above 90%, single-photon purities above 94% and first-lens brightnesses above 45% are reached for all pulse lengths. The use of longer pulses allows for a slightly higher first-lens brightness, but with a slight degradation of the single photon purity

due to re-excitation. The extracted single-photon indistinguishability is maintained approximately constant for all pulse lengths. For a pulse duration of 22 ps we obtain a first-lens brightness of $B_{\text{FL}} = 0.51 \pm 0.01$, with $g^{(2)}(0) = 0.061 \pm 0.001$, $M_s = 0.915 \pm 0.003$. The brightness is more than a factor of two greater than one observed on the same sample using resonant excitation in a cross-polarization configuration [6]. It corresponds to a detected count rate of 6 MHz using a 69% efficient single photon detector and a laser repetition rate of 81 MHz, which is limited by the low optical transmission of 17% of our experimental set-up. Considering the extraction efficiency of our cavities $\eta_{\text{ext}} \approx 0.65$, and the theoretically expected $p_{\text{QD}}^{\text{LA}} \approx 0.85$ (see Supplementary Material), the maximum expected first-lens brightness is $B_{\text{FL}} \lesssim 0.55$, very close to our experimental observation. We note that by improving the spectral filtering we would be able to operate at even smaller detunings, enabling higher occupation probabilities to be reached.

In conclusion, we have reported on a new approach to bring QD-based single photon sources closer to deterministic operation. Our approach relies on the very general property that neutral excitons in quantum dots naturally present linearly-polarized dipoles. Remarkably, the use of phonon-assisted excitation enables near-unity photon indistinguishability and high occupation probability. We note that the use of the exciton linear dipole could also be applied to the recent proposition of dichromatic excitation scheme [23, 36]. However the use of phonon-assisted excitation enables a significant gain in stability and robustness, since the scheme is resilient to drifts in QD-laser detuning and excitation power. All these features are of great importance for practical applications in quantum technologies. Finally, the use of unpolarized cavities and the possibility of exciting and collecting the photons in all polarization directions could also be applied to the four-level structure of a charged exciton, in order to generate photonic cluster states [37].

Acknowledgements. The authors would like to thank Andrew White and Marcelo Pereira de Almeida for experimental help. This work was partially supported by the ERC PoC PhoW, the French Agence Nationale pour la Recherche (grant ANR QuDICE), the IAD - ANR support ASTRID program Projet ANR-18-ASTR-0024 LIGHT, the QuantERA ERA-NET Cofund in Quantum Technologies, project HIPHOP, the French RENATECH network, a public grant overseen by the French National Research Agency (ANR) as part of the "Investissements d'Avenir" programme (Labex NanoSaclay, reference: ANR-10-LABX-0035). J.C.L. and C.A. acknowledge support from Marie SkłodowskaCurie Individual Fellowships SMUPHOS and SQUAPH, respectively. S.C.W. acknowledges support from NSERC (the Natural Sciences and Engineering Research Council), AITF

(Alberta Innovates Technology Futures), and the SPIE Education Scholarships program. H. O. and N. C. acknowledge support from the Paris Ile-de-France Rgion in the framework of DIM SIRTEQ.

Declarations. Niccolo Somaschi and Pascale Senellart are CTO and CSO of Quandela, respectively. All other authors declare no conflicts of interest.

-
- [1] Somaschi, N. et al. Near-optimal single-photon sources in the solid state. *Nature Photonics* **10**, 340–345 (2016). URL <https://doi.org/10.1038/nphoton.2016.23>.
- [2] Ding, X. et al. On-demand single photons with high extraction efficiency and near-unity indistinguishability from a resonantly driven quantum dot in a micropillar. *Phys. Rev. Lett.* **116**, 020401 (2016). URL <https://link.aps.org/doi/10.1103/PhysRevLett.116.020401>.
- [3] Senellart, P., Solomon, G. & White, A. High-performance semiconductor quantum-dot single-photon sources. *Nature Nanotechnology* **12**, 1026–1039 (2017). URL <https://doi.org/10.1038/nnano.2017.218>.
- [4] Wang, H. et al. Boson sampling with 20 input photons and a 60-mode interferometer in a 10^{14} -dimensional hilbert space. *Phys. Rev. Lett.* **123**, 250503 (2019). URL <https://link.aps.org/doi/10.1103/PhysRevLett.123.250503>.
- [5] Wang, H. et al. Towards optimal single-photon sources from polarized microcavities. *Nature Photonics* **13**, 770–775 (2019). URL <https://doi.org/10.1038/s41566-019-0494-3>.
- [6] Ollivier, H. et al. Reproducibility of high-performance quantum dot single-photon sources. *ACS Photonics* **7**, 1050–1059 (2020). URL <https://doi.org/10.1021/acsphtnics.9b01805>.
- [7] Barth, A. et al. Fast and selective phonon-assisted state preparation of a quantum dot by adiabatic undressing. *Physical Review B* **94** (2016).
- [8] Cosacchi, M., Ungar, F., Cygorek, M., Vagov, A. & Axt, V. M. Emission-frequency separated high quality single-photon sources enabled by phonons. *Phys. Rev. Lett.* **123**, 017403 (2019). URL <https://link.aps.org/doi/10.1103/PhysRevLett.123.017403>.
- [9] Gustin, C. & Hughes, S. Efficient pulse-excitation techniques for single photon sources from quantum dots in optical cavities. *Advanced Quantum Technologies* **3**, 1900073 (2020).
- [10] Takemoto, K. et al. Quantum key distribution over 120 km using ultrahigh purity single-photon source and superconducting single-photon detectors. *Scientific Reports* **5**, 14383 (2015). URL <https://doi.org/10.1038/srep14383>.
- [11] Slussarenko, S. & Pryde, G. J. Photonic quantum information processing: A concise review. *Applied Physics Reviews* **6**, 041303 (2019). URL <https://doi.org/10.1063/1.5115814>.
- [12] Wang, J., Sciarrino, F., Laing, A. & Thompson, M. G. Integrated photonic quantum technologies. *Nature Photonics* **14**, 273–284 (2020). URL <https://doi.org/10.1038/s41566-019-0532-1>.
- [13] Rudolph, T. Why i am optimistic about the silicon-photonic route to quantum computing. *APL Photonics* **2**, 030901 (2017). URL <https://doi.org/10.1063/1.4976737>.
- [14] Ramelow, S. et al. Highly efficient heralding of entangled single photons. *Opt. Express* **21**, 6707–6717 (2013). URL <http://www.opticsexpress.org/abstract.cfm?URI=oe-21-6-6707>.
- [15] Weston, M. M. et al. Efficient and pure femtosecond-pulse-length source of polarization-entangled photons. *Opt. Express* **24**, 10869–10879 (2016). URL <http://www.opticsexpress.org/abstract.cfm?URI=oe-24-10-10869>.
- [16] Kaneda, F., Garay-Palmett, K., U'Ren, A. B. & Kwiat, P. G. Heralded single-photon source utilizing highly nondegenerate, spectrally factorable spontaneous parametric downconversion. *Opt. Express* **24**, 10733–10747 (2016). URL <http://www.opticsexpress.org/abstract.cfm?URI=oe-24-10-10733>.
- [17] Spring, J. B. et al. Chip-based array of near-identical, pure, heralded single-photon sources. *Optica* **4**, 90–96 (2017). URL <http://www.osapublishing.org/optica/abstract.cfm?URI=optica-4-1-90>.
- [18] Francis-Jones, R. J. A., Hoggarth, R. A. & Mosley, P. J. All-fiber multiplexed source of high-purity single photons. *Optica* **3**, 1270–1273 (2016). URL <http://www.osapublishing.org/optica/abstract.cfm?URI=optica-3-11-1270>.
- [19] Xiong, C. et al. Active temporal multiplexing of indistinguishable heralded single photons. *Nature Communications* **7**, 10853 (2016). URL <https://doi.org/10.1038/ncomms10853>.
- [20] Joshi, C., Farsi, A., Clemmen, S., Ramelow, S. & Gaeta, A. L. Frequency multiplexing for quasi-deterministic heralded single-photon sources. *Nature Communications* **9**, 847 (2018). URL <https://doi.org/10.1038/s41467-018-03254-4>.
- [21] Kaneda, F. & Kwiat, P. G. High-efficiency single-photon generation via large-scale active time multiplexing. *Science Advances* **5** (2019).
- [22] Meyer-Scott, E., Silberhorn, C. & Migdall, A. Single-photon sources: Approaching the ideal through multiplexing. *Review of Scientific Instruments* **91**, 041101 (2020). URL <https://doi.org/10.1063/5.0003320>.
- [23] He, Y.-M. et al. Coherently driving a single quantum two-level system with dichromatic laser pulses. *Nature Physics* **15**, 941–946 (2019). URL <https://doi.org/10.1038/s41567-019-0585-6>.
- [24] He, Y.-M. et al. On-demand semiconductor single-photon source with near-unity indistinguishability. *Nature Nanotechnology* **8**, 213–217 (2013). URL <https://doi.org/10.1038/nnano.2012.262>.
- [25] Wu, Y. et al. Population inversion in a single ingaas quantum dot using the method of adiabatic rapid passage. *Phys. Rev. Lett.* **106**, 067401 (2011). URL <https://link.aps.org/doi/10.1103/PhysRevLett.106.067401>.
- [26] Wei, Y.-J. et al. Deterministic and robust generation of single photons from a single quantum dot with 99.5% indistinguishability using adiabatic rapid passage. *Nano Letters* **14**, 6515–6519 (2014). URL <https://doi.org/10.1021/nl503081n>.
- [27] Tomm, N. et al. A bright and fast source of coherent single photons (2020). arXiv 2007.12654.

- [28] Bayer, M. et al. Fine structure of neutral and charged excitons in self-assembled in(ga)as/(al)gaas quantum dots. *Phys. Rev. B* **65**, 195315 (2002). URL <https://link.aps.org/doi/10.1103/PhysRevB.65.195315>.
- [29] Glässl, M., Barth, A. M. & Axt, V. M. Proposed robust and high-fidelity preparation of excitons and biexcitons in semiconductor quantum dots making active use of phonons. *Phys. Rev. Lett.* **110**, 147401 (2013). URL <https://link.aps.org/doi/10.1103/PhysRevLett.110.147401>.
- [30] Quilter, J. H. et al. Phonon-assisted population inversion of a single ingaas/gaas quantum dot by pulsed laser excitation. *Phys. Rev. Lett.* **114**, 137401 (2015). URL <https://link.aps.org/doi/10.1103/PhysRevLett.114.137401>.
- [31] Léger, Y., Besombes, L., Maingault, L. & Mariette, H. Valence-band mixing in neutral, charged, and mn-doped self-assembled quantum dots. *Phys. Rev. B* **76**, 045331 (2007). URL <https://link.aps.org/doi/10.1103/PhysRevB.76.045331>.
- [32] Kowalik, K., Krebs, O., Lemaître, A., Gaj, J. A. & Voisin, P. Optical alignment and polarization conversion of the neutral-exciton spin in individual inas/gaas quantum dots. *Phys. Rev. B* **77**, 161305 (2008). URL <https://link.aps.org/doi/10.1103/PhysRevB.77.161305>.
- [33] Ollivier, H. et al. Hong-ou-mandel interference with imperfect single photon sources (2020). arXiv 2005.01743.
- [34] Grange, T. et al. Reducing phonon-induced decoherence in solid-state single-photon sources with cavity quantum electrodynamics. *Phys. Rev. Lett.* **118**, 253602 (2017). URL <https://link.aps.org/doi/10.1103/PhysRevLett.118.253602>.
- [35] Reindl, M. et al. Highly indistinguishable single photons from incoherently excited quantum dots. *Phys. Rev. B* **100**, 155420 (2019). URL <https://link.aps.org/doi/10.1103/PhysRevB.100.155420>.
- [36] Koong, Z. X. et al. Coherent dynamics in quantum emitters under dichromatic excitation (2020). arXiv 2009.02121.
- [37] Lindner, N. H. & Rudolph, T. Proposal for pulsed on-demand sources of photonic cluster state strings. *Phys. Rev. Lett.* **103**, 113602 (2009). URL <https://link.aps.org/doi/10.1103/PhysRevLett.103.113602>.
- [38] Hilaire, P. et al. Deterministic assembly of a charged quantum dot-micropillar cavity device (2019). 1909.02440.
- [39] Esmail Zadeh, I. et al. Single-photon detectors combining high efficiency, high detection rates, and ultra-high timing resolution. *APL Photonics* **2**, 111301 (2017). URL <https://doi.org/10.1063/1.5000001>.

METHODS

Devices We study two samples, referred to as Sample A and B, each of which contain several devices consisting of a QD deterministically located at the center of an electrically connected micropillar cavity [1]. The quality factor of the cavities on Sample A (B) is around 4000 (10000), and the cavities are almost circular: they exhibit only a small degree of polarization, with two linearly-polarized cavity modes typically separated by $\approx 70 \mu\text{eV}$ ($\approx 30 \mu\text{eV}$), which is much smaller than the cavity linewidth of $\approx 300 \mu\text{eV}$ ($\approx 150 \mu\text{eV}$).

Experimental Set-up. To excite the QD via LA-assisted excitation we require a pulse that is blue-detuned from the QD resonance by $0.3 - 0.8 \text{ nm}$. We start with a 3 ps pulsed Ti-Sapphire laser with a central wavelength around 924 nm and a 81 MHz repetition rate. The laser spectrum is shaped using a 4-f filtering system to obtain pulses with tunable temporal length from 3 ps to 22 ps and negligible spectral overlap with the QD emission at 924.82 nm. The co-linearly polarized single photons are collected with a non-polarizing beam-splitter transmitting 90% of the light. Three high-transmission ($\sim 95\%$ each), 0.8 nm FWHM, high-extinction band-pass filters (Alluxa) separate the single photons from the excitation laser. A half and quarter waveplate are used to precisely align the polarization along the exciton axis (X or Y) inside the cavity. Superconducting nanowire single photon detectors (SNSPDs) with 25-30 ps timing jitter and an efficiency of 75% at low count rates, and 69% at the maximum measured count rate, are used to record the time dependence of the emission and the second order intensity correlations.

Measuring Linear Dipoles To measure the emission from the two linear dipoles of the neutral exciton, we add a polarizer to the output and measure the signal in cross-polarisation to the input light. By rotating the HWP on the input, we can change the angle of the linear polarization of the excitation light. When the polarization of the laser is orthogonal to one of the dipoles, say Y , then only the X dipole is excited and the quantum dot only emits X -polarized light. Since we are collecting in cross-polarisation we do not collect any signal, and there is a minimum in the collected light. When the light excites a general linear combination of the two dipoles, then the quantum dot can emit light into the orthogonal polarisation [6]. As the angle of polarization is rotated, we see minima in the signal when the light excites only one dipole, and maxima in the signal when we excite an equal superposition of the two dipoles, as shown in Figure 1(c).

Single-photon purity and indistinguishability. To measure the single-photon purity we use a Hanbury Brown-Twiss set-up, where the collected photons from a source are incident on a 50:50 beam splitter and correlations between the two outputs are measured. The proportion of coincident clicks at zero time delay compared to the uncorrelated peaks gives the second-order autocorrelation, $g^{(2)}(0)$, which is related to the single-photon purity $P = 1 - g^{(2)}(0)$. To measure the indistinguishability of the output we perform Hong-Ou-Mandel interference between subsequently emitted photons from the source. The photon train is separated at a beam splitter and one arm is delayed by the pulse separation time. Two subsequently emitted photons are simultaneously incident at a second beam splitter, and undergo quantum interference. The visibility of this interference, V_{HOM} , together with the second-order autocorrelation of the input, $g^{(2)}(0)$, gives access to the indistinguishability of the single-photon component of each wavepacket, M_s , via $M_s = (V_{\text{HOM}} + g^{(2)}(0)) / (1 - g^{(2)}(0))$ [33].

Supplementary Material

Parameters controlling the source brightness

The brightness of a QD source is determined by a subtle combination of many parameters. Firstly, p_{QD} , quantifies the occupation probability of the exciton state of the quantum dot at the end of the excitation pulse. Considering the near unity quantum efficiency of quantum dot optical transitions, it also reflects the probability that one photon is emitted by the QD per pulse. In practice, p_{QD} can be reduced by blinking phenomena or imperfect population inversion [38]. Secondly, the extraction efficiency η_{ext} is determined by two factors. On one hand, the QD emits a single photon into the cavity mode with probability $\beta = F_p/(F_p + \gamma)$, (where F_p is the Purcell factor into the mode, and γ is the emission rate into all other modes normalized to the nominal rate). On the other hand, the out-coupling efficiency η_{out} then gives the probability that a photon exits the desired cavity mode and reaches the collection lens. Accordingly, $\eta_{\text{ext}} = \beta \eta_{\text{out}}$. Finally, the polarization efficiency η_{pol} describes the fraction of polarized single photon emission that can be collected in a given scheme. The polarized first lens brightness is thus $\mathcal{B}_{\text{FL,pol}} = \beta \eta_{\text{out}} p_{\text{QD}} \eta_{\text{pol}}$. In our system the extraction efficiency $\eta_{\text{ext}} = \beta \eta_{\text{out}} \approx 0.65$, independent of the excitation scheme. For RF excitation in a mostly unpolarized cavity, one obtains a polarization efficiency of $\eta_{\text{pol}} < 0.5$, whereas for the phonon-assisted excitation, it is $\eta_{\text{pol}} = \frac{1}{2}(1 + D_{\text{LP}})$, and can be as high as 0.997 as demonstrated here.

Occupation probability of LA-assisted excitation

A detailed theoretical model for estimating the efficiency of LA-phonon-assisted excitation is given in [9]. We apply this model with the relevant experimental parameters in order to understand how the brightness of the polarized single photon source depends on the detuning and pulse duration of the excitation pulse.

The results of the simulation are given in Fig. S.1, and show the maximum occupation probability, p_{QD} , maximised over excitation power, for a given detuning and pulse duration. The maximum occupation probability depends both on the detuning and on pulse length [9]. More precisely, it depends on the ratio of the excitation pulse duration to the lifetime of the two-level system, and for long enough pulses compared to the transition lifetime, the maximum occupancy has little dependence on the detuning. For our system, we can see that for pulse durations of around 19 ps and longer, the occupation probability is high and approximately constant for detunings between 0.3 and 1.0 nm. The maximum occupation probability is approximately 0.85 less efficient than for resonant excitation. This was the case for the measurements shown in Fig. 2 that were obtained on Sample B presenting a higher Purcell factor, hence reduced lifetime. In contrast, in Fig. 3 we explored neutral excitons in Sample A which present lower Purcell factors, and we observed a slight dependence with detuning for our limited region of pulse lengths.

We note that the above theoretical approach is valid for a two level system: it applies perfectly to the case of the linear dipole of a neutral exciton under parallel excitation, but also to the case of the charged exciton when excitation and collection are cross-polarized. However, further modeling would be required if exciting a combination of the two exciton dipoles instead. Indeed, this would result in a complex excitation/emission dynamics within the three level system $\{|g\rangle, |X\rangle, |Y\rangle\}$ [6] that is expected to significantly modify the phonon-assisted excitation process and cannot be compared to the case of a two-level system [7].

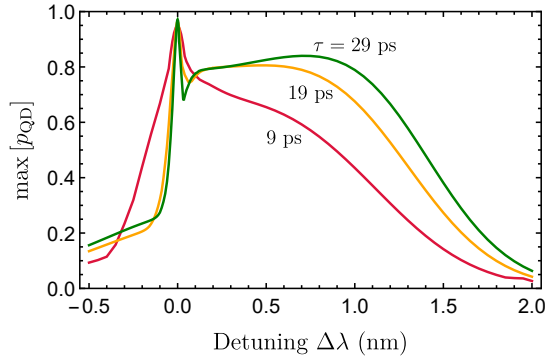


FIG. S.1. Simulated occupation probability p_{QD} numerically maximized over excitation power for a fixed Gaussian pulse FWHM duration τ . For the simulation we assumed a quantum dot with a natural lifetime of $1/\gamma = 1$ ns at 8 K coupled to a cavity mode with a lifetime of $1/\kappa = 32$ ps by the cavity coupling given by $1/g = 100$ ps corresponding to a Purcell factor of $F_p = 12.8$.

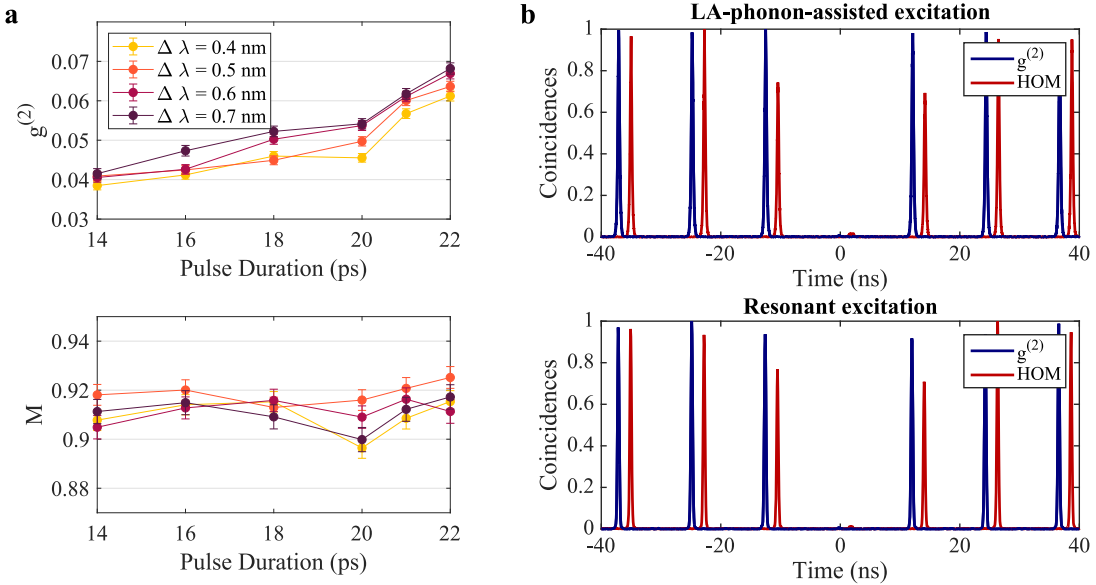


FIG. S.2. (a) The second-order autocorrelation $g^{(2)}(0)$ (upper) and the single-photon indistinguishability, M_s , (lower) as a function of the detuning ($\Delta\lambda$) and pulse duration (τ) of LA-phonon-assisted excitation. For each point, the values are obtained for a power maximizing the occupation probability. (b) Measured $g^{(2)}(0)$ (blue) and HOM interference (red) for LA-phonon-assisted excitation (upper) and resonant excitation (lower), when a 10 pm etalon is added to the collection path.

Single-Photon Purity and indistinguishability

To investigate the single-photon purity when using phonon-assisted excitation, we measure the second-order autocorrelation, $g^{(2)}(0)$, as a function of the excitation pulse duration and detuning from resonance. For each set of parameters, the excitation power was adjusted to maximise the single-photon emission. Figure S.2(a) shows that the $g^{(2)}(0)$ increases for longer pulse durations, indicating that there is an increasing probability of re-excitation. For a pulse duration greater than 14 ps we can deduce that re-excitation is a significant cause of the non-zero $g^{(2)}(0)$. However, it is not clear what limits the $g^{(2)}(0)$ to around 4% for shorter pulse durations. The single-photon indistinguishability is constant across these range of parameters, as shown in the lower panel of Figure S.2(a).

When a 10 pm bandwidth etalon is added to the set-up to provide additional spectral filtering of the collected photons, the $g^{(2)}(0)$ and HOM visibility improve significantly as shown in Figure S.2(b).

We note that it is theoretically predicted that phonon-assisted excitation should enhance the single-photon purity as compared to resonant excitation, since the phonon-induced relaxation process leads to a delay in photon emission and hence suppresses the probability of re-excitaiton [8]. This suppression should become more significant when the lifetime of the quantum dot is comparable to the phonon-relaxation timescale. By exploring the large parameter space of available detunings, pulse durations, and Purcell factors to adjust the optimal QD emission lifetimes, it may be possible to achieve significantly higher single-photon purity under LA-phonon-assisted excitation.

Loss Budget

We measure the transmission of the optical components of our set-up using a continuous wave laser centered at the quantum dot emission wavelength, 924.82 nm, and details are given in Table S.1. To measure the transmission of the window of the cryostation and the objective lens, we measure the reflection of the beam off the flat diode surface of the sample, and assume that the reflectivity of the surface is 100% in order to give an upper bound on the transmission of the optical elements. The light passes through the cryostation window, the objective lens and two waveplates twice, and we give the single-pass transmission of these combined elements in Table S.1.

The transmission of the filters is less than the maximum of 95% per filter, since we angle-tune the filters to fully suppress the excitation laser. The filters were aligned here for an excitation laser with a detuning of $\Delta\lambda = 0.8 \text{ nm}$ and a pulse duration of $\tau = 20 \text{ ps}$. In order to calculate the first lens brightness at a different detuning or pulse duration, the filters are aligned to suppress the laser and then the relative transmission efficiency is measured with respect to this known point.

The detector efficiency of the SNSPDs at a fixed bias current depends on the count rate because of the dead time of the detectors [39]. We measured the detection efficiency using an attenuated laser pulse with a repetition rate of 81 MHz. The detection efficiency for a low count rate of 500 kHz was found to be 75%. However, when the count rate increases to 6 MHz the detection efficiency decreases to 69%, as shown in Figure S.3. We note that this may not be the optimal detection efficiency

for these parameters as we did not adjust the bias current of the SNSPDs.

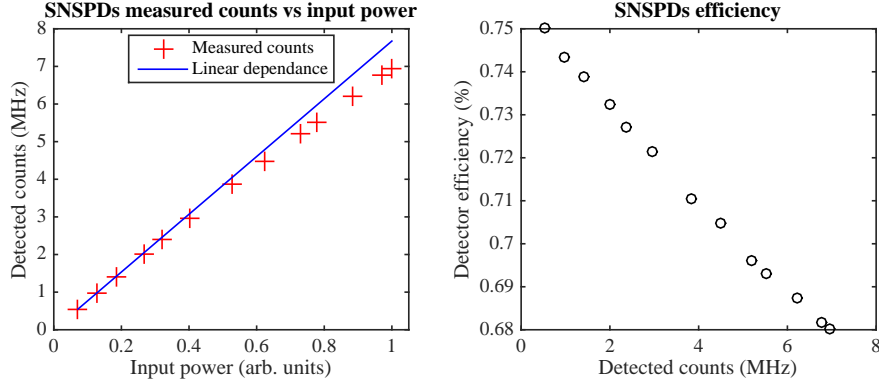


FIG. S.3. Left: Detected counts on an SNSPD as a function of the input power. Right: Detection efficiency of SNSPD as a function of the detected count rate.

The total efficiency of the set-up for a detuning of $\Delta\lambda = 0.8$ nm, a pulse duration of $\tau = 20$ ps, and a detected count rate of $R_{\text{det}} = 6$ MHz is $\eta = 0.17 \pm 0.01$. The repetition rate of the laser $R_L = 81$ MHz, and therefore this corresponds to a first lens brightness of $B_{\text{FL}} = R_{\text{det}}/(R_L \times \eta) = 0.44$ for these parameters.

Element	Transmission
Cryostat Window + Objective Lens + QWP + HWP	0.80 ± 0.02
Beam splitter	0.92 ± 0.01
5 Mirrors	0.95 ± 0.01
Telescope	0.98 ± 0.01
2 Waveplates	0.95 ± 0.01
3 Bandpass filters	0.64 ± 0.02
Fibre coupling efficiency	0.60 ± 0.02
Detection efficiency (low count rate)	0.75 ± 0.03
Detection efficiency (6 MHz detected rate)	0.69 ± 0.03

TABLE S.1. **Loss Budget.** The transmission of optical elements in the set-up, and efficiency of the superconducting nanowire detectors